Geology

Interplate earthquakes as a driver of shallow subduction erosion

Kelin Wang, Yan Hu, Roland von Huene and Nina Kukowski

Geology 2010;38;431-434
doi: 10.1130/G30597.1

Notes

Interplate earthquakes as a driver of shallow subduction erosion

Kelin Wang[1,2]*, Yan Hu[2], Roland von Huene[3], and Nina Kukowski[4]
[1]Pacific Geoscience Centre, Geological Survey of Canada, 9860 West Saanich Road, Sidney, British Columbia V8L 4B2, Canada
[2]School of Earth and Ocean Sciences, University of Victoria, Victoria, British Columbia V8P 5C2, Canada
[3]Department of Geology, University of California–Davis, Davis, California 96616, USA
[4]Deutsches GeoForschungsZentrum (GFZ Potsdam), Telegrafenberg, D-14473 Potsdam, Germany

ABSTRACT

Basal erosion is a prevalent process at subduction zones and plays an important role in the mass balance of global plate tectonics. In contradiction with the theoretical expectation that basal erosion requires high basal friction and hence compression in the upper plate, extensional faulting is commonly observed in submarine wedges that undergo such erosion. Here we propose a model to explain this apparent paradox in terms of stress fluctuations during earthquake cycles. In this model, basal erosion occurs during large earthquakes when the shallow, rate-strengthening part of the plate interface strengthens and its overlying wedge weakens, but extension occurs during interseismic relaxation of wedge stress. The mechanics of basal erosion provide important information on the nature of the updip limit of the megathrust seismogenic zone in margins dominated by basal erosion.

INTRODUCTION

Subduction erosion occurs at many convergent margins, resulting in seafloor subsidence and landward migration of the trench axis and volcanic arc (von Huene and Scholl, 1991; Clift and Vannucchi, 2004). Basal erosion is a process of continuing removal of materials from the underside of the upper plate by the subducting plate. In some cases, the eroded materials may be underplated back to the upper plate at greater depths (Collot et al., 2008). Figure 1A summarizes essential features of end-member erosion-dominated subduction zones such as northern Chile (Sallarès and Ranero, 2005; von Huene et al., 2009), Peru (Clift et al., 2003; Krabbenhöft et al., 2004), Costa Rica (Ranero and von Huene, 2000), Ecuador (Sage et al., 2006), Kuril (Klaeschen et al., 1994), and northeast Japan (von Huene et al., 1994).

In the middle prism (Fig. 1A), under a sediment cover, are crystalline basement or older sedimentary rocks that are fractured predominantly by deep-cutting normal faults. As basal erosion proceeds, small incremental motion of these faults accompanies gradual subsidence of the seafloor. Erosion in the middle prism area is the focus of this paper, although basal erosion may also occur further downdip, along the seismogenic zone of the plate interface and at the base of the overriding mantle wedge (Kukowski and Oncken, 2006; Tonarini et al., 2007). The very front part of the upper plate is a frontal prism that consists of sediments and rock debris and retains a quasi-constant size (von Huene et al., 2004). For simplicity, we neglect the usually small frontal prism in the following discussions, so that the middle prism can be represented by the wedge model shown in Figure 1B.

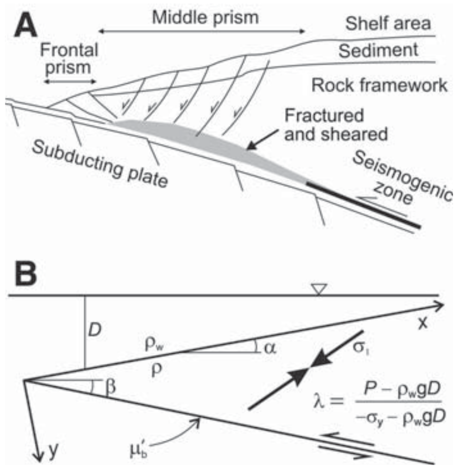

Figure 1. A: Schematic illustration of shallow part of margins dominated by subduction erosion (based on von Huene et al., 2004). B: Coulomb wedge model for middle prism showing coordinate system (x, y), maximum compressive stress σ_1, surface slope angle α, basal dip β, and definition of pore fluid pressure ratios λ. σ_y is normal stress in y direction, ρ and ρ_w are densities of wedge material and overlying water of depth *D*, respectively, and g is gravitational acceleration.

The mechanics of shallow basal erosion have been enigmatic because of the conflicting information on the strength of the basal fault. On the one hand, basal erosion theoretically requires a strong basal fault relative to the strength of the wedge material. On the other hand, the prevalence of deep-cutting extensional faults in the middle prism indicates a very weak basal fault. In this paper we propose a model of reconciliation by considering variations of the fault strength during subduction earthquake cycles.

DIFFICULTY WITH CONSTANT FAULT STRENGTH

The Coulomb wedge theory (Davis et al., 1983; Dahlen, 1984) is recognized to be the most appropriate theory that describes the first-order mechanics of subduction zone prisms. The theory shows that, if the wedge is in a critical state, that is, everywhere at Coulomb failure, its taper angle is determined by the relative strengths of the wedge material and basal fault. For the purpose of explaining essential concepts, it suffices to consider the simple model of a uniform noncohesive wedge. A measure of the strength of a noncohesive wedge is $\mu(1 - \lambda)$, where μ is the coefficient of internal friction and λ is the pore fluid pressure ratio (defined in Fig. 1B) quantifying the effect of the pressure of interstitial fluid within the wedge. The effective coefficient of basal friction μ_b' (Fig. 1B) depends on both the friction coefficient μ_b and pore fluid pressure along the fault zone. If a basal pore fluid pressure ratio λ_b similar to λ in physical meaning is defined (Wang et al., 2006), μ_b' can be expressed as $\mu_b' = \mu_b(1 - \lambda_b)$. Given geometry and strength, a thrust wedge has two critical states depending on basal friction: an extensionally critical state (i.e., gravitational collapse) if the basal friction is sufficiently low (Fig. 2A) and a compressively critical state if the basal friction is sufficiently high (Fig. 2C). For intermediate basal friction, the wedge is in a stable state and deforms only elastically (Fig. 2B).

The existence of a basal fault means $\mu_b' < \mu(1 - \lambda)$, that is, the fault is weaker than the wedge material. If $\mu_b' = \mu(1 - \lambda)$, there is no mechanical distinction between the two, and one of the two conjugate sets of potential failure planes (plastic slip lines) is parallel with the basal fault (Fig. 2D). This is the ideal state of basal erosion. The basal fault cannot become any stronger, because the bottom of the wedge will yield and shear, resulting in basal erosion (Dahlen, 1984). In real subduction zones, basal erosion represents a mechanical state close to the ideal state, that is, $\mu_b' \approx \mu(1 - \lambda)$. It requires one or both of the two conditions: (1) a relatively strong fault, and (2) relatively weak wedge material, particularly the wedge material in proximity to the fault.

While a strong fault has been invoked to explain basal erosion (e.g., Adam and Reuther, 2000), the predicted stresses within the wedge (Fig. 2D) are inconsistent with the extensional

*E-mail: kwang@nrcan.gc.ca.

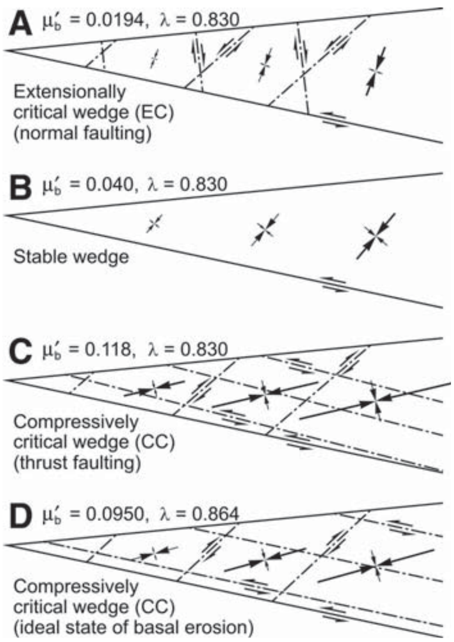

Figure 2. State of stress obtained using solutions of Wang and Hu (2006) for uniform noncohesive Coulomb wedge with surface slope angle $\alpha = 5.5°$ and basal dip $\beta = 12°$, representative of middle prism at northern Chile (Sallarès and Ranero, 2005). Converging arrows represent principal stresses, with the larger pair being σ_1. Coefficient of internal friction μ is assumed to be 0.7, but exact value is not crucial because of its trade-off with the internal pore fluid pressure ratio λ in controlling strength of wedge material $\mu(1 - \lambda)$. A: Extensionally critical (EC) state. This is a thrust wedge collapsing under its own weight and is not to be confused with extensional wedge overlying a normal fault. B: Stable state in which only elastic deformation takes place. C: Compressively critical (CC) state. D: Ideal state of basal erosion, a special CC state. In A, C, and D, dot-dashed lines are plastic slip lines (potential failure planes).

faulting commonly observed in the middle prism (Fig. 1A). Regardless of the history of the normal faults, they currently reflect a state of stress represented by Figure 2A, which would indicate a weak basal fault. The condition of a weak wedge can be brought about by elevated pore fluid pressure; for example, the wedge shown in Figure 2D is weaker than that in Figure 2A because of a higher λ value. The idea of a wedge weakened at its base by elevated pore fluid pressure has been invoked to explain basal erosion (von Huene et al., 2004; Ranero et al., 2008). However, in the scenario of steady subduction, such fluid pressure will also weaken the plate interface fault and thus not be able to facilitate basal erosion, especially if we consider that the source of the fluid is the subducted sediment or igneous crust beneath the wedge.

PROPOSED MODEL

We argue that the concept of dynamic Coulomb wedge proposed by Wang and Hu (2006) for accretionary prisms can also be applied to basal erosion. The key is the variation of stress and fluid pressure in earthquake cycles. The basal fault is weak and the middle prism is relatively strong in the interseismic period, but strengthening of the basal fault and hydraulic weakening of the prism can both occur during large earthquakes. With this mechanism, erosion of the base of the middle prism does not occur continuously but in brief episodes of coseismic and immediate postseismic deformation. Stress fluctuations must also occur at time scales much longer than earthquake cycles for other reasons, such as changes in the roughness and trench sediment amount on the incoming seafloor. However, earthquakes are the most common mechanism to cause large fluctuations.

Rate-Strengthening Behavior of the Plate Interface Beneath the Middle Prism

If a distinct décollement persists, the updip end of the rate-weakening seismogenic zone may be limited by a range of thermally controlled petrological and hydrological processes (Moore and Saffer, 2001). However, when the basal erosion condition of $\mu_b' \approx \mu(1 - \lambda)$ prevails, there will not be a single fault plane, but only a constantly modified cataclastic shear zone (Fig. 1A), which may mix with subducting sediments to maintain a subduction channel (Calahorrano et al., 2008; Vannucchi et al., 2008). Deformation in this shear zone should be dominated by distributed shear with granularization and comminution, and the inability to localize shear strongly discourages seismic rupture and sets an updip limit to the seismogenic zone. This is similar to the presence of granular fault gouge leading to rate strengthening at shallow depths of continental faults (Marone, 1998).

For erosional margins, the seismogenic zone for the most part is landward of the middle prism (Fig. 1A). This is evident by a simple comparison of bathymetry and the many well-located megathrust earthquakes off northeast Japan (Yamanaka and Kikuchi, 2004). Another well-studied example showing the location of the seismogenic zone is the 1995 Antofagasta earthquake in northern Chile (Sobiesiak et al., 2007). While the seismogenic zone undergoes a stress drop during an earthquake, the shallow segment (shear zone) beneath the middle prism undergoes a stress increase. Along this shallow segment, coseismic slip decreases updip toward the trench, and negative stress drop leads to postseismic afterslip. If the shallow shear zone occasionally permits shear localization and coseismic rupture very close to the trench, the slip rate is expected to be slower; this should result in longer source duration, as reported for this type of margin (Bilek and Lay, 2002). In the following, the shallow interface shear zone is modeled as a single frictional contact.

Alternation of Stress in the Wedge Between Compression and Tension

During an interseismic period when the seismogenic zone is locked and has little displacement, the updip part of the fault also has little motion except for a phase of postseismic slip immediately following the previous earthquake. The very low or zero slip rate results in a low μ_b' along the shallow segment due to its rate-strengthening behavior. The overlying middle prism thus is in a stable state (Fig. 2B) or an extensionally critical state (Fig. 2A). During an earthquake, the seismogenic zone undergoes a stress drop. However, as the upper plate bounces seaward, the strength of the rate-strengthening updip segment suddenly increases to resist the rupture. This process of stress transfer was numerically modeled in Wang and He (2008) and Hu and Wang (2008), and it was shown that the stress increase in the shallow segment is of the order of a few megapascals for typical seismogenic zone stress drops. The coseismic μ_b' increase of the shallow segment causes compression in the overlying middle prism and may drive it into a compressively critical state (Fig. 2C). Pore fluid pressure in a compressed wedge will also increase, and the middle prism can be suddenly weakened by the fluid pressure pulse. This is opposite of what happens along the underlying fault zone, in which dilatancy that accompanies rate strengthening (Marone, 1998) decreases pore fluid pressure. If λ is raised to a critical value, the wedge approaches the ideal state of basal erosion (Fig. 2D).

Reconciling Basal Erosion and Extensional Faulting

Although the stress solutions shown in Figure 2 are derived using an analytical solution (Wang and Hu, 2006) that assumes a uniform wedge, the illustrated basic principle applies to real wedges of nonuniform strength. When a wedge is driven into failure by an earthquake (Fig. 2D), it is the weakest part that fails. There is ample evidence to suggest that the weakest part of the middle prisms is their base because of elevated pore fluid pressure due to the release of water from the subducting sediment and oceanic crust (von Huene et al., 2004; Ranero et al., 2008). If the basal part is weaker than the average strength assumed for Figure 2, the condition of $\mu_b' \approx \mu(1 - \lambda)$ can be locally met by an increase in μ_b' that is smaller than shown in Figure 2D. As a consequence of shear failure occurring predominantly at the base, there is little permanent compressive deformation in the rest of the middle prism, such as reverse reactivation of the normal faults.

After the seismogenic zone again becomes locked, continuing shear deformation of the shallow interface beneath the middle prism results in afterslip and serves to transport the shear-zone material farther downdip. Small rate-weakening patches embedded in this overall rate-strengthening segment may rupture to produce aftershocks during the afterslip. As the shallow segment weakens due to the decreasing slip rate, the overlying middle prism gradually relaxes into a stable state (Fig. 2B). If μ_b' becomes very low, the middle prism will further relax into an extensionally critical state, favoring extensional faulting (Fig. 2A). In contrast to the coseismic wedge failure that occurs as basal erosion, interseismic tension affects the entire wedge and may cause the existing normal faults to move. These normal faults show very small total displacements over geological time scales (Ranero and von Huene, 2000); this probably indicates that their motion is infrequent. It is reasonable to expect the middle prism to reach the extensionally critical state only occasionally, that is, once in many earthquake cycles, because this state requires rather extreme stress relaxation.

CONDITIONS FOR BASAL EROSION

Only four examples of many possible states of the middle prism in earthquake cycles are shown in Figure 2. The curve dividing stable and unstable regions in Figure 3A shows λ and μ_b' values of other possible critical states for this wedge. During a large earthquake, the middle prism moves from a stable or extensionally critical state to the upper right direction, toward a stronger basal fault and weaker wedge. The line of $\mu_b' = \mu(1 - \lambda)$ is tangent to the critical-state curve at the ideal state of basal erosion, a graphical illustration that the ideal state is the only critical state in which the basal fault is as strong as the wedge. This figure also shows that the condition of $\mu_b' \approx \mu(1 - \lambda)$ prevails in a relatively wide range of compressively critical states in the neighborhood of the ideal state, and hence basal erosion occurs rather readily. In fact, $\mu_b' \approx \mu(1 - \lambda)$ in the compressively critical state shown in Figure 2C.

For comparison, we show a similar diagram in Figure 3B for an accretionary prism with geometry similar to a section of the Nankai subduction zone shown by Park et al. (2002). This geometry is typical of prisms at margins dominated by sediment accretion, with the surface slope and basal dip being gentler than the middle prisms of erosion-dominated margins. Figure 3B illustrates that basal erosion for this wedge geometry would require a much higher pore fluid pressure ratio, and $\mu_b' \approx \mu(1 - \lambda)$ only for a very narrow range of compressively critical states. Therefore, basal erosion tends not to occur in accretionary prisms unless conditions are unusual.

A fundamental point in the above mechanism of basal erosion is that ultimate strength of the plate interface under the middle prism is limited only by the coseismic strength of the basal part of the wedge, $\mu(1 - \lambda)$. This is consistent with the roughness of the downgoing plate of erosion-dominated margins (Fig. 1A).

The long-term geometry of the middle prism is regulated by its own strength that is ultimately controlled by the prevailing λ during earthquakes. To explain this, we extend Figure 3A into an α-λ-μ_b' space (Fig. 4) by spanning other surface slope angles (α) but still holding the basal dip (β) fixed at 12° for simplicity. Figure 4 shows that basal erosion will occur more readily if the surface slope is higher because it does not require as high a pore fluid pressure ratio. If α is low and the coseismic λ is not high enough to bring the wedge to near the ideal state of basal erosion, the wedge will be pushed into a compressively critical state such as state A in Figure 4 (a situation similar to Fig. 2C except for a smaller α), and μ_b' will continue to increase. The wedge thus becomes unstable (above the critical surface) and must rapidly deform to increase its surface slope. Over many earthquake cycles, the wedge will acquire a higher surface slope (state B), so that basal erosion occurs more readily. The wedge will eventually be adjusted to have an optimal slope that allows the wedge to stay near the ideal state of basal erosion appropriate for the prevailing λ. This explains the observation that the middle prism surface slope of erosional margins tends to be greater than at accretionary margins (Clift and Vannucchi, 2004; Hu and Wang, 2008). Along-strike variations in surface slope can be explained by systematic variations in fluid pressure and basal stress.

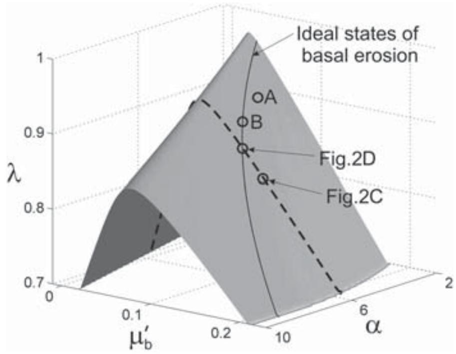

Figure 4. Critical-state surface in α-λ-μ_b' space for noncohesive wedges with basal dip β = 12° and μ = 0.7. Three axes α, λ, and μ_b' represent three basic elements of this mechanical system: wedge geometry, wedge strength, and fault strength, respectively. Stable region is under surface. Ideal states of basal erosion (solid line on surface) are subset of compressively critical (CC) states. Dashed line is the same curve as shown in Figure 3A, for which surface slope angle α = 5.5°.

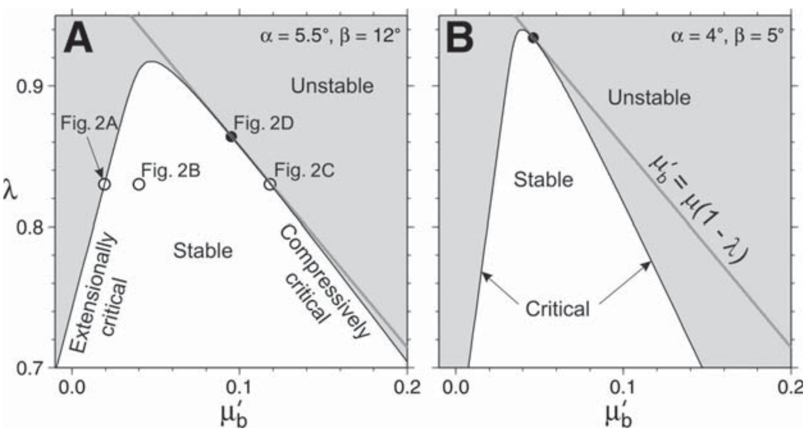

Figure 3. A: Critical values of pore fluid pressure ratio λ and basal friction μ_b' for wedge shown in Figure 2. All extensionally critical states form left limb of critical-state curve, and all compressively critical (CC) states form right limb. Stable region is under curve (white). Straight-line tangent to critical-state curve at ideal state of basal erosion (solid circle) represents condition $\mu_b' = \mu(1 - \lambda)$; α—surface slope angle; β—basal dip. B: Similar to A, but for wedge geometry representative of accretionary prisms at accretion-dominated margins.

FUTURE OBSERVATIONS

Some predictions of this model can be tested with future observations. The presence of a shear zone beneath the middle prism has been inferred only from seismic observations and laboratory experiments on granular fault gouges. The plate interface may be directly sampled via deep sea drilling. Stress relaxation of the wedge is expected to be faster right after the rupture zone of a large megathrust earthquake becomes locked. The accompanying afterslip of the shallow plate interface and its duration can be constrained using seafloor deformation monitoring. To date, the only direct seafloor global positioning system measurement along an erosional margin was off Peru (Gagnon et al., 2005), and it showed no detectable motion of the updip segment 30 yr after an earthquake. Active normal faulting during the relaxation may be constrained by repeat high-resolution near-bottom seafloor mapping, and its seismic signal, if any, can be detected using ocean bottom seismographs and downhole seismic observatory. Pore fluid pressure in the wedge is predicted to increase during an earthquake but decrease afterward. Fluid pressure in the interface shear zone may show the opposite, that is, an increase during interseismic "healing" but decrease during coseismic dilatancy. These can be tested using seafloor borehole observatories (Davis et al., 2009).

ACKNOWLEDGMENTS

We thank J.Y. Collot for discussions and reviewing an earlier version of the manuscript and three anonymous reviewers for insightful comments. Hu is supported by a National Sciences and Engineering Research Council of Canada graduate scholarship. This is Geological Survey of Canada contribution 20090309.

REFERENCES CITED

Adam, J., and Reuther, C.D., 2000, Crustal dynamics and active fault mechanics during subduction erosion: Application of frictional wedge analysis on to the North Chilean forearc: Tectonophysics, v. 321, p. 297–325, doi: 10.1016/S0040-1951(00)00074-3.

Bilek, S.L., and Lay, T., 2002, Tsunami earthquakes possibly widespread manifestations of frictional conditional stability: Geophysical Research Letters, v. 2, no. 14, 1673, doi: 10.1029/2002GL015215.

Calahorrano, A., Sallares, V., Collot, J.-Y., Sage, F., and Ranero, C.R., 2008, Nonlinear variations of the physical properties along the southern Ecuador subduction channel: Results from depth-migrated seismic data: Earth and Planetary Science Letters, v. 267, p. 453–467, doi: 10.1016/j.epsl.2007.11.061.

Clift, P.D., and Vannucchi, P., 2004, Controls on tectonic accretion versus erosion in subduction zones: Implications for the origin and recycling of the continental crust: Review of Geophysics, v. 42, RG2001, doi: 10.1029/2003RG000127.

Clift, P.D., Pecher, I., Kukowski, N., and Hampel, A., 2003, Tectonic erosion of the Peruvian forearc, Lima Basin, by subduction and Nazca Ridge collision: Tectonics, v. 22, no. 3, doi: 10.1029/2002TC001386.

Collot, J.-Y., Agudelo, W., Ribodetti, A., and Marcaillou, B., 2008, Origin of a crustal splay fault and its relation to the seismogenic zone and underplating at the erosional north Ecuador–south Colombia oceanic margin: Journal of Geophysical Research, v. 113, B12102, doi: 10.1029/2008JB005691.

Dahlen, F.A., 1984, Noncohesive critical Coulomb wedges: An exact solution: Journal of Geophysical Research, v. 89, p. 10,125–10,133, doi: 10.1029/JB089iB12p10125.

Davis, D.M., Suppe, J., and Dahlen, F.A., 1983, Mechanics of fold-and-thrust belts and accretionary wedges: Journal of Geophysical Research, v. 88, p. 1153–1172.

Davis, E.E., Becker, K., Wang, K., and Kinoshita, K., 2009, Co-seismic and post-seismic pore-fluid pressure changes in the Philippine Sea plate and Nankai decollement in response to a seismogenic strain event off Kii Peninsula, Japan: Earth, Planets, and Space, v. 61, p. 649–657.

Gagnon, K., Chadwell, C.D., and Norabuena, E., 2005, Measuring the onset of locking in the Peru-Chile trench with GPS and acoustic measurements: Nature, v. 434, p. 205–208, doi: 10.1038/nature03412.

Hu, Y., and Wang, K., 2008, Coseismic strengthening of the shallow portion of the subduction fault and its effects on wedge taper: Journal of Geophysical Research, v. 113, B12411, doi: 10.1029/2008JB005724.

Klaeschen, D., Belykh, I., Gnibidenko, H., Patrikeyev, S., and von Huene, R., 1994, Structure of the Kuril Trench from seismic reflection records: Journal of Geophysical Research, v. 88, no. B12, p. 24,173–24,188, doi: 10.1029/94JB01186.

Krabbenhöft, A., Bialas, J., Kopp, H., Kukowski, N., and Hübscher, C., 2004, Crustal structure of the Peruvian continental margin from wide-angle seismic studies: Geophysical Journal International, v. 159, p. 749–764, doi: 10.1111/j.1365-246X.2004.02425.x.

Kukowski, N., and Oncken, O., 2006, Subduction erosion—The "normal" mode of forearc material transfer along the Chilean margin?, *in* Oncken, O., et al., eds., The Andes: Active subduction orogeny: Berlin, Springer-Verlag, p. 217–236.

Marone, C., 1998, Laboratory-derived friction laws and their application to seismic faulting: Annual Review of Earth and Planetary Sciences, v. 26, p. 649–696, doi: 10.1146/annurev.earth.26.1.643.

Moore, J.C., and Saffer, D., 2001, Updip limit of the seismogenic zone beneath the accretionary prism of southwest Japan: An effect of diagenetic to low grade metamorphic processes and increasing effective stress: Geology, v. 29, p. 183–186, doi: 10.1130/0091-7613(2001)029<0183:ULOTSZ>2.0.CO;2.

Park, J.O., Tsuru, T., Kodaira, S., Cummins, P.R., and Kaneda, Y., 2002, Splay fault branching along the Nankai subduction zone: Science, v. 297, p. 1157–1160.

Ranero, C.R., and von Huene, R., 2000, Subduction erosion along the Middle America convergent margin: Nature, v. 404, p. 748–755, doi: 10.1038/35008046.

Ranero, C.R., Grevemeyer, I., Sahling, H., Barckhausen, U., Hensen, C., Wallmann, K., Weinrebe, W., Vannucchi, P., von Huene, R., and McIntosh, K., 2008, The hydrogeological system of erosional convergent margins and its influence on tectonics and interplate seismogenesis: Geochemistry Geophysics Geosystems, v. 9, no. 3, Q03S04, doi: 10.1029/2007GC001679.

Sage, F., Collot, J.-Y., and Ranero, C.R., 2006, Interplate patchiness and subduction-erosion mechanisms: Evidence from depth-migrated seismic images at the central Ecuador convergent margin: Geology, v. 34, p. 997–1000, doi: 10.1130/G22790A.1.

Sallarès, V., and Ranero, C.R., 2005, Structure and tectonics of the erosional convergent margin off Antofagasta, north Chile (23°30′S): Journal of Geophysical Research, v. 110, B06101, doi: 10.1029/2004JB003418.

Sobiesiak, M., Meyer, U., Schmidt, S., Götze, H.-J., and Krawczyk, C.M., 2007, Asperity generating upper crustal sources revealed by *b* value and isostatic residual anomaly grids in the area of Antofagasta, Chile: Journal of Geophysical Research, v. 112, B12308, doi: 10.1029/2006JB004796.

Tonarini, S., Agostini, S., Doglioni, C., Innocenti, F., and Manetti, P., 2007, Evidence for serpentinite fluid in convergent margin systems: The example of El Salvador (Central America) arc lavas: Geochemistry Geophysics Geosystems, v. 8, Q09014, doi: 10.1029/2006GC001508.

Vannucchi, P., Remitti, F., and Bettelli, G., 2008, Geological record of fluid flow and seismogenesis along an erosive subducting plate boundary: Nature, v. 451, p. 699–703, doi: 10.1038/nature06486.

von Huene, R., and Scholl, D.W., 1991, Observations at convergent margins concerning sediment subduction, erosion, and the growth of continental crust: Reviews of Geophysics, v. 29, p. 279–316, doi: 10.1029/91RG00969.

von Huene, R., Klaeschen, D., and Cropp, B., 1994, Tectonic structure across the accretionary and erosional parts of the Japan Trench margin: Journal of Geophysical Research, v. 99, no. B11, p. 22,349–22,361, doi: 10.1029/94JB01198.

von Huene, R., Ranero, C.R., and Vannucchi, P., 2004, Generic model of subduction erosion: Geology, v. 32, p. 913–916, doi: 10.1130/G20563.1.

von Huene, R., Ranero, C.R., and Scholl, D.W., 2009, Convergent margin structure in high-quality geophysical images and current kinematic and dynamic models, *in* Lallemand, S., and Funiciello, F., eds., Subduction zone geodynamics: Berlin, Springer-Verlag, 137–157.

Wang, K., and He, J., 2008, Effects of frictional behavior and geometry of subduction fault on coseismic seafloor deformation: Seismological Society of America Bulletin, v. 98, p. 571–579, doi: 10.1785/0120070097.

Wang, K., and Hu, Y., 2006, Accretionary prisms in subduction earthquake cycles: The theory of dynamic Coulomb wedge: Journal of Geophysical Research, v. 111, B06410, doi: 10.1029/2005JB004094.

Wang, K., He, J., and Hu, Y., 2006, A note on pore fluid pressure ratios in the Coulomb wedge theory: Geophysical Research Letters, v. 33, L19310, doi: 10.1029/2006GL027233.

Yamanaka, Y., and Kikuchi, M., 2004, Asperity map along the subduction zone in northeastern Japan inferred from regional seismic data: Journal of Geophysical Research, v. 109, B07307, doi: 10.1029/2003JB002683.

Manuscript received 5 August 2009
Revised manuscript received 2 December 2009
Manuscript accepted 4 December 2009

Printed in USA